ACS APPLIED MATERIALS & INTERFACES

Research Article

www.acsami.org

Mixed Ionic/Electronic Conducting Surface Layers Adsorbed on Colloidal Silica for Flow Battery Applications

Jeffrey J. Richards,[†] Austin D. Scherbarth,[†] Norman J. Wagner,[‡] and Paul D. Butler*[,†,‡]

[†]NIST Center for Neutron Research, National Institute of Standards and Technology, Gaithersburg, Maryland 20899, United States

[‡]Department of Chemical and Biomolecular Engineering, University of Delaware, Newark, Delaware 98195, United States

Supporting Information

ABSTRACT: Slurry based electrodes have shown promise as an energy dense and scalable storage technology for electrochemical flow batteries. Key to their efficient operation is the use of a conductive additive which allows for volumetric charging and discharging of the electrochemically active species contained within the electrodes. Carbon black is commonly used for this purpose due to the relatively low concentrations needed to maintain electrical percolation. While carbon black supplies the desirable electrical properties for the application, it contributes detrimentally to the rheology characteristics of these concentrated suspensions. In this work, we develop a synthesis protocol to produce inorganic oxide particles with electrostatically adsorbed poly(3,4-ethylenedioxithiophene):polystyrenesulfonate (PEDOT:PSS). Using a combination of small angle neutron scattering (SANS), electron microscopy, and thin-film conductivity, we show that the synthesis scheme provides a flexible platform to form conductive PEDOT:PSS-SiO_2 nanoparticle dispersions. Based on these measurements, we demonstrate that these particles are stable when dispersed in propylene carbonate. Using a combination of rheology and dielectric spectroscopy, we show that these stable dispersions facilitate electrical percolation at concentrations below their mechanical percolation threshold, and this percolation is maintained under flow. These results demonstrate the potential for strategies which seek to decouple mechanical and electrical percolation to allow for the development of higher performance conductive additives for slurry based flow batteries.

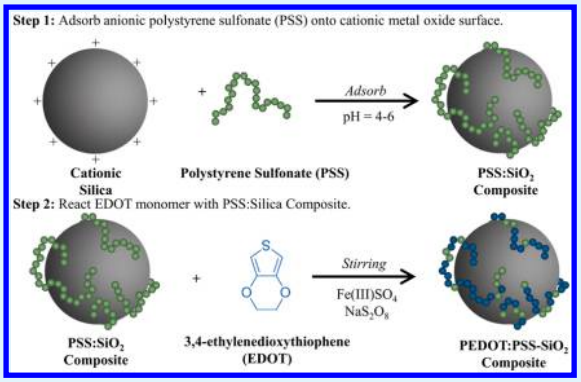

KEYWORDS: *composite, nanoparticle, small angle neutron scattering, flow battery, rheology*

INTRODUCTION

The development of flow batteries promises economic storage of grid-scale renewable energy.[1] To this end, slurry based flowable electrodes have recently gained interest to significantly improve the power density as compared to flow batteries containing soluble electrolytes.[2,3] The operation of slurry based electrochemical storage technologies requires the maintenance of good electrical conductivity throughout the flowing electrode during the course of charging/discharging cycles.[4,5] Conducting carbon based materials are ubiquitous in this application due to their performance, availability, and low cost. However, their attractive interparticle potential in dispersion results in high viscosities. Thus, while these networks of carbon black particles allow for electrical percolation at relatively low particle loadings (less than 0.05 volume fraction of the electrolyte in some cases), the rheological properties of slurries that incorporate carbon materials severely limit the practical realization of flowable slurry based electrolytes. The energetic costs of continuously pumping these viscous slurries can exceed 20% of the storage capacity of the battery.[6] Further, the addition of carbon black to the slurries so as to provide electrical percolation comes at the cost of reducing the energy storage density.

In order to circumvent the limitations of carbon black materials, we have synthesized poly(3,4-ethylenedioxithiophene):polystyrenesulfonate (PEDOT:PSS) adsorbed surface layers on colloidal particles. We hypothesize that these surface layers will not only provide the necessary electrical conductivity for a conductive additive in flowable electrodes, but also provide enhanced colloidal stability that will improve slurry rheological performance in polar solvents with respect to carbon black. The PEDOT:PSS complex consists of electrically conductive PEDOT conjugated polymer doped by the sulfonate groups on the PSS backbone.[7] This complex therefore possesses the ability to conduct both ionic and electronic charge. Additionally, polystyrenesulfonate is a strong polyanion that can impart electrosteric stability to colloidal dispersions. Prior work has shown that electrosteric stabilization of nanoparticles can provide significant benefits to the rheological performance of dense particulate slurries.[8,9] PEDOT:PSS thin films have also been shown to possess extremely high electrical conductivities, exceeding 200 S/cm. Therefore, it is possible

Received: June 17, 2016
Accepted: August 18, 2016
Published: August 18, 2016

DOI: 10.1021/acsami.6b07372
ACS Appl. Mater. Interfaces 2016, 8, 24089−24096

that this surface layer can be engineered to have sufficient conductivity to exceed the electrical performance of the commonly used carbon black.

In this work, we develop a synthetic scheme to create PEDOT−PSS:SiO_2 composite nanoparticles using a simple electrostatic adsorption strategy to demonstrate proof of concept on a common nanoparticle substrate, silica nanoparticles. We characterize the morphology of this PEDOT:PSS layer as a function of its composition using a combination of electron microscopy and small angle neutron scattering. From these measurements, we quantify the degree of solvation of the PEDOT:PSS surface layer and identify attributes of these adsorbed surface layers that contribute to the overall colloidal stability and the dispersion's electrical conductivity. Finally, we show that these nanoparticles can be formulated into stable dispersions capable of maintaining electrical conductivity while in the fluid phase.

RESULTS AND DISCUSSION

1. Synthesis of PEDOT:PSS-SiO_2 Particles. The strength of adsorption of a polyelectrolyte to an oppositely charged surface is dependent on its persistence length, its linear charge density, its molecular weight, as well as the charge density and radius of curvature of the surface.[10,11] Once adsorbed, its conformation is determined by the balance between the favorable ionic attraction and the entropic penalty of the adsorbed polymer. On a flat surface, the polyelectrolyte adopts a conformation on the surface that maximize the number of ionic interactions. As the radius of curvature of the surface decreases, the conformation of the polyelectrolyte becomes more extended as a result of entropic considerations leading to a greater prevalence of chain "tails" and "loops" extending from the surface.[11] These tails facilitate bridging flocculation for colloid/polyelectrolyte complexes.[12] In order to avoid bridging flocculation, we examined the characteristics of the PSS-SiO_2 association as a function of PSS molecular weight at a fixed ionic strength using model cationic SiO_2 particles (Klebosol, 30 CAL 50 AZ Electronics, Lamotte, France). These particles have a proprietary surface coating and are positively charged as supplied with a point of zero charge measured to be at pH 10.0 and nominal size, R_p = 40.5 nm. The results of these measurements and analysis are summarized in SI Figures S.1−3. Briefly, we find that there is strong association of the PSS to the cationic silica particles. This association leads to different extents of bridging flocculation, some of which can be mitigated using sonication to shear disperse the particles to form stable PSS-SiO_2 composites. The conditions for which flocculation of the PSS-SiO_2 complex is minimized are low-molecular-mass PSS and large PSS-SiO_2 ratio (i.e., when there is a large excess of PSS).

Measurements of the zeta potential of the bare silica particles in a pH range between 4 and 6 reported in Figure 1 correspond to a surface charge density of 1.71 ± 0.24 $\mu C/cm^2$. Also shown in Figure 1, upon adsorption of PSS, the surface charge switches sign and the magnitude of the apparent zeta potential corresponds to a surface charge density of −2.71 ± 0.19 $\mu C/cm^2$ in acidic conditions. The appearance of this "overcharging" phenomenon is consistent with the presence of "tails" and "loops" that extend away from the particle surface.[13] The DLS and SANS measurements from the PSS-SiO_2 particles shown in Figure S.4 allow us to conclude that these dispersions consist of primarily monomeric silica particles with a small proportion of dimers. Using the surface area of the bare silica particles, the

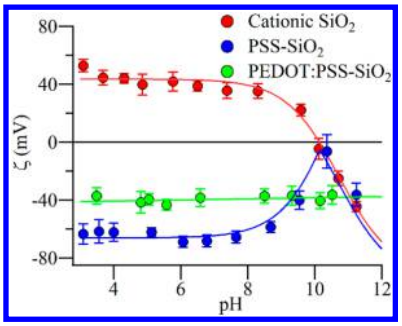

Figure 1. Apparent zeta potential (mV) vs pH for Klebosol, PSS-SiO_2 composite particles, and PEDOT:PSS-SiO_2. All samples measured in 0.005 mol/L KCl. Lines are included to guide the eye. Error bars derived from standard deviation calculated by the average of multiple runs.

apparent surface charge on the PSS:SiO_2 particles corresponds to an adsorbed mass, Γ_{PSS} = 0.6 mg/m^2 assuming 0.20 mole fraction dissociation of sulfate groups.[14] As can be seen in Figure 1, the negative surface charge of PSS-SiO_2 particles is pH dependent, and in basic conditions, the PSS-SiO_2 complex can be dissociated and the native charge on the silica particles restored. The PSS-SiO_2 particle complexes are stable as a dispersion for months when the solution is maintained in acidic conditions.

To initiate the polymerization of EDOT to poly(3,4-ethylenedioxithiophene), iron(III) sulfate is added as a catalyst and sodium persulfate an oxidant, is added to drive the PEDOT:PSS complexation. Before synthesis, a stock solution is prepared that contains PSS content far in excess of that necessary to saturate the surface charge. Therefore, there is a bulk PEDOT:PSS complexation reaction occurring at the same time as the PEDOT:PSS-SiO_2 complexation. The synthesis is initiated when the desired quantity of EDOT is added to the mixture and the reaction is allowed to evolve over the course of a 24 h period to completion. This is sufficient to fully consume the EDOT monomer. Over the course of the synthesis, the samples transition to a dark blue color, consistent with the polymerization and doping of PEDOT to the PEDOT:PSS complex. After the synthesis, the resulting particles are extensively washed to remove residual catalyst, salts, and unassociated PEDOT:PSS from the particles using a protocol outlined in the Materials and Methods section. Using this protocol, stable PEDOT:PSS layers on the surface of the SiO_2 particles can be isolated. Unlike the adsorbed PSS layers, these composite layers are robust against centrifugation and pH changes, as indicated by a constant negative charge over the entire pH range as shown in Figure 1.

UV−visible absorption spectroscopy measurements of PEDOT:PSS-SiO_2 nanoparticles are shown in Figure 2a. The color of the suspension shows a clear blue tint (inset photo) and the broad absorption feature in the near-infrared region of the absorbance profile is consistent with the presence of PEDOT:PSS. After removing the contribution from the turbidity resulting from the SiO_2 particles by subtracting a power-law slope of Absorbance $\sim \lambda^{-4}$, where λ is the wavelength, the absorption features of both the PEDOT and PSS become evident. Polystyrenesulfonate has a strong absorbance at 5.3 eV and, because of the extensive washing procedure employed in this study, can only be present on the particle surface complexed with the PEDOT. Figure 2b shows energy-dispersive X-ray spectroscopy (EDS) measurements

DOI: 10.1021/acsami.6b07372
ACS Appl. Mater. Interfaces 2016, 8, 24089−24096

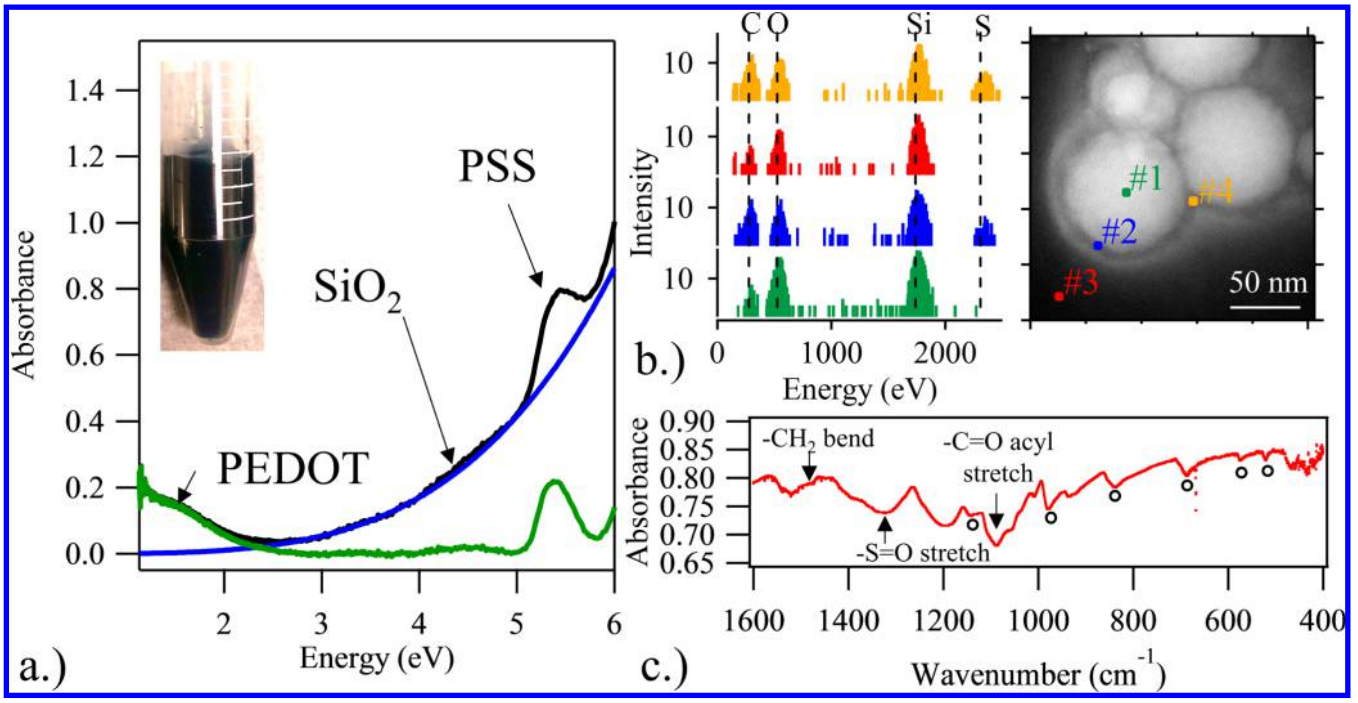

Figure 2. (a) UV−visible spectroscopy of PEDOT:PSS/SiO_2 nanoparticles; inset is a photograph of vial containing PEDOT:PSS/SiO_2 nanoparticles. (b) STEM EDS map of PEDOT:PSS-SiO_2 particles. (c) FTIR spectra from PEDOT:PSS/SiO_2 particles.

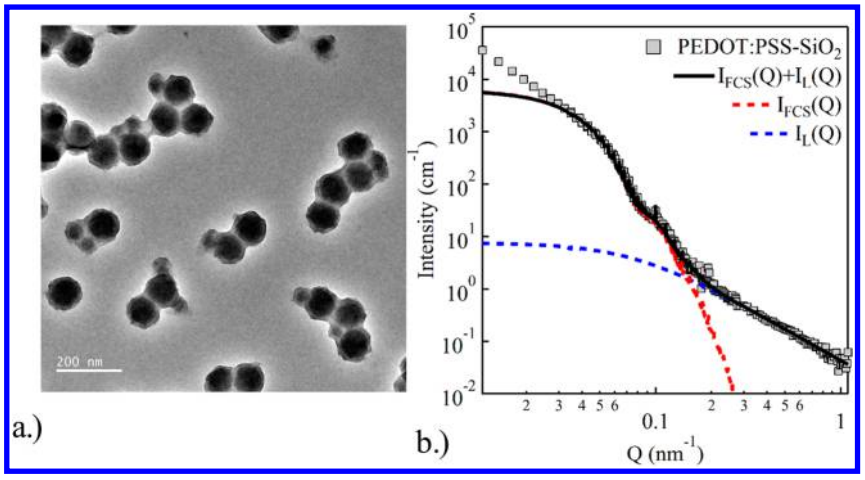

Figure 3. (a) Representative TEM image of PEDOT:PSS-SiO_2 nanoparticles after synthesis and wash steps. (b) SANS measurement from PEDOT:PSS-SiO_2 showing the components of the model that takes into account hydration of solvent shell and polymer structure factor within the shell. IFCS(Q) and IL(Q) are the two components of the model that account for fuzziness of the interface and the polymer correlations within the adsorbed layer respectively.

obtained from a STEM micrograph taken of dried particles. The EDS measurements confirm the robust adsorption of PEDOT:PSS to the particle's surface as indicated by the polymer film visible on the silica surface containing both carbon and sulfur. In addition, FTIR spectra of the dried particles show spectral features associated with polaron and bipolaron transitions for doped PEDOT (indicated by the circles in Figure 2c) along with characteristic absorption features associated with PSS.

This synthesis scheme proves to be a flexible route to forming PEDOT:PSS-SiO_2 particles as the reaction conditions allow the molar ratio of EDOT to PSS to be systematically changed. We anticipate that both the morphological and rheological characteristics of PEDOT:PSS-SiO_2 particles will be determined by the molar ratio of EDOT to sulfonate (SO_4^{-2}) on the PSS backbone. The molar ratio of EDOT monomer to styrenesulfonate monomer (EDOT:SO_4^{-2}) determines the hydrophobicity of the PEDOT:PSS complex with increasing PEDOT content leading to reduced solution stability. At high EDOT:SO_4^{-2} ratios, PEDOT:PSS syntheses have been observed to gel. For bulk PEDOT:PSS, it is also known that the EDOT:SO_4^{-2} ratio determines the PEDOT:PSS complex conductivity with increasing EDOT content leading to higher conductivities.[7] In order to characterize the effect on the EDOT:SO_4^{-2} ratio on the stability and morphological properties of PEDOT:PSS-SiO_2 suspensions, additional experiments were performed for varying adsorbed layer composition as described next.

2. Structural Characterization of PEDOT:PSS-SiO_2 Particles. To study the effect of varying layer composition, a

DOI: 10.1021/acsami.6b07372
ACS Appl. Mater. Interfaces 2016, 8, 24089−24096

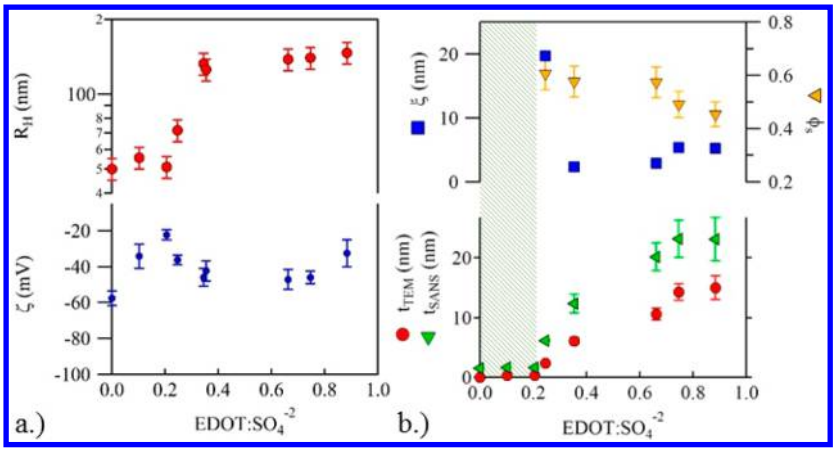

Figure 4. (a) Zeta potential and hydrodynamic radius of particles as a function of EDOT:SO_4^{-2} ratio. (b) Results of analysis of TEM/SANS measurements of PEDOT:PSS film thickness on SiO_2 particles. The green hatched region demarcates the area where there is no polymer coat visible in the TEM micrographs. Error bars on both plots represent 1 standard deviation from the average value stated.

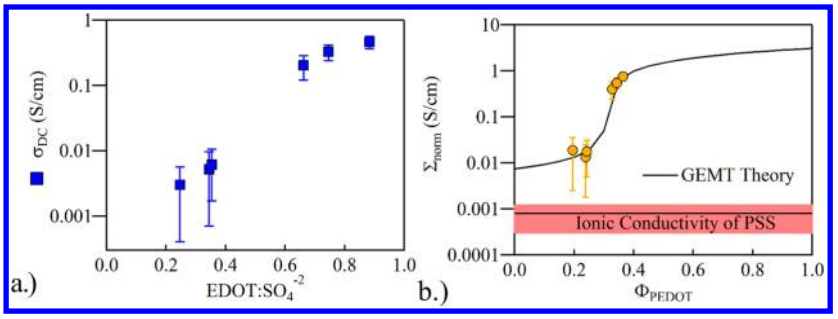

Figure 5. (a) Conductivity, σ, measured from thin films of PEDOT:PSS-SiO_2 particles. (b) Normalized thin-film conductivity, Σ_{norm}, as a function of volume fraction of PEDOT within the PEDOT:PSS layer, Φ_{PEDOT}, estimated from the molar ratio included in the synthesis. Error bars are 1 standard deviation of five devices tested for each particle type.

number of PEDOT:PSS:SiO_2 particles were prepared as a function of EDOT:SO_4^{-2} ratio. In order to characterize the PEDOT:PSS-SiO_2 particles, we performed transmission electron microscopy (TEM) and small angle neutron scattering (SANS) measurements. A representative micrograph and SANS spectrum are shown in Figure 3a,b for a 0.01 mass fraction PEDOT:PSS:SiO_2 dispersion prepared by reacting EDOT with PSS at a 0.9:1 molar EDOT:SO_4^{-2} ratio. The TEM in Figure 3a shows that the PEDOT:PSS:SiO_2 particles consist of a silica core decorated with a conformally coated polymer shell. Note that there is a small fraction of smaller particles in the dispersion as supplied, which are also evident in Figure 3a. The shell thickness is conserved even in the particle aggregates suggesting that the particles are fully dispersed prior to coating. Aggregates typically form as a result of TEM sample preparation, which required drying, while some small number of aggregates may exist in solution due to bridging flocculation.

The SANS data is fit to a scattering model developed to describe the distribution of polymer around the silica core that accounts for density fluctuations within the polymer layer. The details of the model are summarized in the Supporting Information, but the model follows a similar approach to Pederson et al. where a fuzzy interface is used to account for the radial decay of scattering length density within the polymer layer and a Lorentz term is used to account for the polymer correlations.[15] The contributions from the two components are plotted in Figure 3b. The scattering spectra of each sample and parameters extracted from the model fits are summarized in the Supporting Information (Figure S.4 and Table S.1). The deviation at low-Q of the SANS spectrum is consistent with the TEM micrograph as a distribution of dimers, trimers, and higher number density aggregates in these dispersions results in a power-law slope instead of Guinier plateau as predicted by the model.[16−18] These results are also consistent with the hydrodynamic diameter extracted from DLS experiments of these samples in D_2O shown in Figure 4a.

Figure 4b contains the results from the TEM and SANS analysis. As Figure 4b reveals, the molar EDOT:SO_4^{-2} ratio has a significant influence on the apparent thickness of the PEDOT:PSS film on the surface of the silica particles. At very low EDOT:SO_4^{-2} ratios, little permanent adsorption is observed and the only clear indication of the presence of a film is from the negative surface charge of the silica indicating the presence of a strongly adsorbed PSS layer. As the molar EDOT:SO_4^{-2} ratio is increased above 0.2, a conformal PEDOT:PSS film appears and grows to a maximum dry size of 15 nm. Fits to the SANS curves corroborate the TEM results, but the thickness parameters extracted from the SANS data are consistently larger than that determined by TEM. We attribute this apparent increase in film thickness to hydration within the PEDOT:PSS layer. The hydration of the PEDOT:PSS layer is also evidenced by the scattering length densities extracted from the model fits and the presence of the high-Q scattering feature accounting for the interchain structure factor within the polymer layer. This structure factor would not be present without the presence of water within the surface layer. The increase in the polymer correlation length, ξ, and decrease in the volume fraction of water, ϕ_s, within the film

DOI: 10.1021/acsami.6b07372
ACS Appl. Mater. Interfaces 2016, 8, 24089−24096

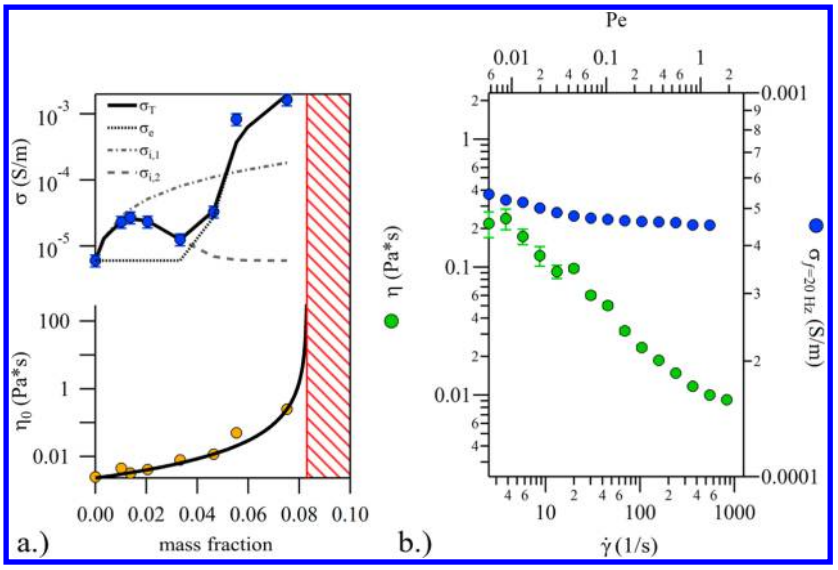

Figure 6. (a) Conductivity, σ (S/m), top, and the zero shear viscosity, η (Pa*s), bottom, versus mass fraction of PEDOT:PSS-SiO_2 particles in propylene carbonate; and (b) viscosity, η (Pa*s), and conductivity, σ (S/m), at f = 20 Hz, versus shear rate, $\dot{\gamma}$ (1/s), for the 0.075 mass fraction PEDOT:PSS sample in propylene carbonate. The red hatched region in (a) is the critical mass fraction estimated from a fit to the Maron-Pierce model. The conductivity models include the conductivity assuming constant counterion dissociation, $\sigma_{i,1}$, an exponentially decreasing fraction of dissociated counterions, $\sigma_{i,2}$, Kirkpatrick's electrical conductivity percolation model, σ_e, and the total $\sigma_T = \sigma_e + \sigma_{i,2}$. The error bars represent 1 standard deviation from the average.

corresponds well with the fact that, after the film has grown to its final size, the further incorporation of PEDOT within the PEDOT:PSS layer drives water out as the environment becomes increasingly hydrophobic.

3. Electrical Characterization of PEDOT:PSS-SiO_2 Particles. The DLS, TEM, and SANS results suggest that the origin of the apparent increase in size is due to interparticle aggregation with aggregate size growing with increasing EDOT:SO_4^{-2}. Nonetheless, the apparent thickness of the adsorbed layer and its degree of solvation are consistent with the growth of a distinct coating of PEDOT:PSS layer on the surface of silica nanoparticles. The growth in thickness of the film is proportional to the amount of EDOT added during the synthesis, suggesting that the film formation mechanism relies on the amount of EDOT available to the reaction and recruitment of bulk PEDOT:PSS to the surface of the silica particles. Consequently, the greater the amount of PSS present in the reaction, the thicker the film that can potentially be formed for a fixed EDOT:SO_4^{-2} ratio. Via this mechanism, a conformal coating of PEDOT:PSS is established surrounding the silica nanoparticles whose properties determine the colloidal stability of the PEDOT:PSS-SiO_2 complex. Particles that have EDOT:SO_4^{-2} ratios exceeding 0.2 maintain robust PEDOT:PSS coverage that is stable against centrifugation and pH changes and lyophylization.

In order to test the electrical properties of the resulting PEDOT:PSS-SiO_2 nanoparticles, thin-film conductivity measurements were made for each particle and plotted as a function of EDOT:SO_4^{-2} ratio as shown in Figure 5. In order to produce these measurements, PEDOT:PSS-SiO_2 particles were dispersed in 0.5 volume fraction water/isopropyl alcohol and deposited onto patterned ITO substrates. The measured resistances were then converted to conductivity using the known geometry of the patterned electrodes. As is apparent in Figure 5a, the conductivity increases with increasing EDOT:SO_4^{-2} ratio. The origin of this enhanced conductivity is correlated with the growth in PEDOT:PSS film thickness as well as to a potential change in film composition. To determine whether film thickness can account for the improved conductivity, the conductivity was normalized in Figure 5b with respect to the volume fraction of PEDOT:PSS in the composite conductor, $\sum_{norm} = \sigma_{film}(r_{core} + t_{SANS})^3/[(r_{core} + t_{SANS})^3 - r_{core}^3]$, and plotted against the volume fraction of EDOT, Φ_{PEDOT}, in the PEDOT:PSS layer calculated from the known synthesis conditions. Once normalized, the conductivity of PEDOT:PSS agrees well with generalized effective medium theory (GEMT) that accounts for the conductivity of a composite consisting of conducting domains (PEDOT rich regions of the film) embedded within an insulator (PSS rich regions of the film).[19] From fits to GEMT theory, we find that the limiting conductivity below the percolation threshold is 0.0075 S/cm and the limiting conductivity above the threshold is 3.1 S/cm (conductivity of the PEDOT domains). The conductivity achieved here compares favorably with values obtained from highly conductive carbon black and bulk PEDOT:PSS films. The apparent percolation threshold is 0.31 volume fraction PEDOT in the PEDOT:PSS complex assuming that all EDOT added in the synthesis is incorporated and the nonideality factor that accounts for the nonuniform shape of the conducting domains is 1.78. These results show that the change in conductivity observed as a function of EDOT:SO_4^{-2} ratio is dominated by the changing composition within the PEDOT:PSS layer on the silica particle surface. This increase in conductivity also coincides with an increasing correlation length extracted from the Lorentz term.

Based on the results presented, the synthesis procedure is demonstrated to generate PEDOT:PSS:SiO_2 composite nanoparticles that exhibit electronic conductivity and colloidal stability. These particles' properties depend on the composition of the PEDOT:PSS layer and the adsorption scheme outlined here proves effective at allowing for facile tuning of this layers' composition. A critical element underlying this work is the demonstration of improved rheological performance and enhanced stability under flow as compared to carbon black

DOI: 10.1021/acsami.6b07372
ACS Appl. Mater. Interfaces 2016, 8, 24089−24096

suspensions in conditions relevant to a flow battery application. In order to demonstrate this, PEDOT:PSS-SiO_2 dispersions were prepared in propylene carbonate (PC), a polar aprotic solvent often used in flow battery applications for its large dielectric constant and large electrochemical window. The particles are readily dispersed in propylene carbonate and form colloidal dispersions that are stable for days.

In order to demonstrate their potential as flow battery materials, a dilution series was performed where the concentration of particles was systematically reduced from the gel point. The zero shear viscosity and conductivity of this series was then measured. These data are shown in Figure 6a. The PEDOT:PSS-SiO_2 particles maintain stability in propylene carbonate and a fluid consistency is maintained to concentrations exceeding 0.075 mass fraction. Above this concentration, the sample gels. The viscosity of the dispersions follows a typical Maron-Pierce model, $\eta_0 \sim (1 - x/x_{gel})^{-2}$, where x_{gel} = 0.083 mass fraction and corresponds to a liquid to gel transition. Samples above this mass fraction exhibit measurable elasticity. The conductivity, σ, calculated from the resistivity of the sample cell is the sum of the conductivity contribution from dissociation of the PSS counterions into the solvent phase and electronic percolation from particle to particle interactions. As the concentration of particles increases in PC, there is initially a sharp increase in the conductivity from neat propylene carbonate, followed by a plateau in conductivity. The propylene carbonate used in this experiment is equilibrated in air and therefore contains trace amounts of water and CO_2. The initial increase in conductivity in the dilute limit is consistent with the limiting molar conductance of sodium ions (Λ_{Na+} = 9.7 S·mol/cm^2)[20] with a molar fractional dissociation of 0.25 which is plotted as $\sigma_{i,1}$ in Figure 6a. As the concentration of particles increases, there is a significant depression in the measured conductivity from that predicted based on the molar concentration of polystyrenesulfonate associated with the particles.[21] As the chains are attached to the particle surface, we anticipate the main contribution to the conductivity results from the dissociated Na^+ ions. As the particle concentration is enriched, the interparticle polyelectrolyte interaction begins to dominate the concentration dependence of the counterion dissociation over the intraparticle polyelectrolyte chain interaction. The apparent decrease is well described as an exponential decay in the contribution of the conductivity from Na^+ ions plotted as $\sigma_{i,2}$ in Figure 6a. When the concentration of particles exceeds a critical concentration, however, there is an abrupt increase in the conductivity by several orders of magnitude. Such a transition is often associated with the onset of electrical percolation. The electrical percolation threshold, defined by Kirkpatrick as concentration where there exists system spanning bond percolation, x_{elec}, occurs for this system at a concentration of 0.033 weight fraction as extracted by the fit to Kirkpatrick's bond percolation model, $\sigma_e \sim (x - x_e)^p$.[22] The model is overlaid and using p = 1.5, consistent with three-dimensional bond percolation, fits the points above the percolation concentration with a prefactor of 0.50.[22,23] Finally, the sum of the contributions, $\sigma_T = \sigma_e + \sigma_{i,2}$, is included to show that the combined conductivity contributions can adequately describe the dependence of the conductivity of the particle suspensions on concentration. All models include the baseline conductivity measured for neat propylene carbonate used for all dilutions.

For the 0.075 mass fraction sample, the steady-state flow curve is measured simultaneously while performing impedance spectroscopy and the results reported in Figure 6b. The low frequency conductivity, which is associated with interparticle electronic transport resistance, decreases only moderately as the dispersion of PEDOT:PSS-SiO_2 particles transition through their shear-thinning regime. This is consistent with the fact that these dispersions consist of electrostatically stabilized conductors whose primary conduction mechanism arises via dynamic interactions between particles, which are only modestly affected over the range of Peclet number, Pe = $6\pi\eta_s R_p^3/k_B T$, used in this experiment where the primary particle size, R_p = 60 nm, is taken as the sum of the typical PEDOT:PSS film thickness and the silica radius. The concentration series data along with the shear rate dependence of the conductivity suggest that the particles maintain a fluid consistency yet are capable of long-range conduction as a result of dynamic interparticle networks that form in the quiescent state. These are likely facilitated by the reduced surface charge on the particle as a result of enhanced counterion condensation with increasing particle concentration. These transient networks facilitate charge transfer without the need for long-range mechanical percolation and gelation. Via this mechanism, we believe there is promise to produce high conductivity fluid suspensions of conductive particles.

CONCLUSIONS

In this work, PEDOT:PSS is adsorbed on the surface of cationic silica particles. The properties of this adsorbed layer are examined using a combination of several techniques including neutron scattering, electron microscopy, and thin film conductivity measurements. These techniques show that the composition of the PEDOT:PSS layer determines not only its electrical conductivity, but also the state of hydration and particle stability. The synthesis method used in this work shows the ability to vary the PEDOT:PSS ratio within the adsorbed polymer layer. PEDOT:PSS-SiO_2 particles that contain relatively high EDOT:SO_4^{-2} ratios show excellent electrical conductivity and increased hydrophobic character leading to stable particle suspensions in propylene carbonate where the primary particles are weakly flocculated. The performance of these particles in suspension is examined for potential use as a conductive additive for flow battery electrodes by examining their conductivity as a function of concentration in propylene carbonate. Using rheology and conductivity measurements, the electrical percolation threshold is shown to occur below the sol−gel transition suggesting the formation of transient particle networks that facilitate long-range electrical transport without long-range mechanical percolation. Steady flow experiments on these percolated suspensions show that their conductivity is maintained over a wide range of shear rates.

These observations suggest important considerations for the performance of slurry based flow batteries. The viscosity and conductivity of suspensions that incorporate conductive additives are key design parameters in the implementation of these promising electrochemical flow systems. While carbon black provides the necessary electrical percolation for slurry based electrodes, its presence imposes unacceptable rheological constraints on the operation of such devices. In this work, we have developed and demonstrated a scalable synthesis to form PEDOT:PSS layers on the surface of metal oxide particles. The resultant particles can be dispersed in polar solvents such as propylene carbonate, yielding stable nanoparticle dispersions with good flowability and electrical conduction comparable to existing electrolyte slurries yet with lower viscosity. The

DOI: 10.1021/acsami.6b07372
ACS Appl. Mater. Interfaces 2016, 8, 24089−24096

flexibility of our synthesis route in particular allows us to independently tune the conductivity and stability of these PEDOT:PSS-SiO_2 particles as well as potentially their shape and size. Using colloidal design principles, we believe that this approach opens up many new avenues to exploring electrically percolated fluids for next generation flow battery applications.

MATERIALS AND METHODS

The colloidal silica (SiO_2) used in this work was supplied as a commercial cationic silica dispersion (0.3 mass fraction Klebosol 30CAL50, R_{avg} = 40.5 nm AZ Electronic Materials, Luxembourg, GE). The sodium polystyrenesulfonate (PSS) was purchased from Scientific Polymer Products, Inc. (Ontario, NY) with M_w = 5180 g/mol ($Đ$ = 1.13) and >95% sulfonation as determined by the manufacturer. Reagent grade reactants for the PEDOT:PSS reaction (Aldrich, St. Louis, MO) consisted of 3,4-ethylenedioxithiophene (EDOT), iron(III) sulfate dehydrate, and sodium persulfate. All PEDOT:PSS-SiO_2 particles used in this work were derived from the same master solution with the only variation being the mass of EDOT added to the reaction mixture. A dispersion of 0.05 weight fraction Klebosol Silica was prepared by diluting the stock dispersion in 0.005 mol/L KCl at a pH = 4. PSS was then added to a concentration of 0.02 mass fraction. Upon addition of PSS, the complexation of PSS to silica was indicated by an abrupt increase in the turbidity of the dispersion. This dispersion was then sonicated using a Sonics model CV17 250 W Horn Sonicator (Newton, CT) operating at 30% intensity for 10 min in an ice bath. While sonicating, the $Fe(III)SO_4{\cdot}2H_2O$ and $Na_2S_2O_8$ were dissolved to a final concentration of 3×10^{-5} mol/L and 0.04 mol/L, respectively. The resulting stable suspension was then degassed and sparged with nitrogen gas for 30 min. From this master batch, 10 mL quantities were separated and the corresponding amount of EDOT monomer was added. The polymerization reaction was allowed to proceed for 24 h at 25 °C. At the end of the polymerization, the characteristic blue color of PEDOT:PSS was apparent in all reaction mixtures. The resulting particles were then centrifuged and washed using a series of solvents (DI water/isopropyl alcohol/propylene carbonate) to remove excess salt, unreacted monomer, and unassociated PEDOT:PSS. After washing steps, the solvent was then exchanged back to water and the samples lyophilized to a dry powder. The washings proved critical to achieving stable dispersions of PEDOT:PSS-SiO_2 particles in both DI water and propylene carbonate, as well as for significantly improving the conductivity of thin films derived from these particles. This is consistent with the observation that PEDOT:PSS consists of a mixture of free PSS and associated PSS to the PEDOT backbone.[7] This unassociated PSS acts as an insulating layer, but can be removed by selection of an appropriate solvent. Polar aprotic solvents have often been used to improve the conductivity of spin-coated PEDOT:PSS thin films and this is necessary in this work.[24] All statements regarding error unless otherwise stated represent 1 standard deviation from the average value.

Electrophoretic mobility measurements were made using a Brookhaven ZetaPALS dip cell. Measurements were made as a function of pH adjusted with HCl and KOH solutions at a fixed KCl concentration (0.005 mol/L). Zeta potential was calculated using approximate electrokinetic models of Ohshima.[25] All measurements were performed on samples containing 1 mg/mL particles. Dynamic light scattering (DLS) measurements were made using a Wyatt Dynapro Nanostar, θ = 90°. Measurements were performed with a silica concentration of 1 mg/mL unless otherwise stated. Transmission electron microscopy (TEM) was performed at the Center for Nanoscale Science and Technology at NIST, Gaithersburg. Bright field images were acquired with a Gatan Orius digital camera on an FEI Titan 80-300 with 300 kV accelerating voltage on Formvar carbon grids (Ted Pella, Inc.). EDAX was performed in STEM mode using silicon dioxide support films on copper. SANS measurements were performed on the NG7 30m small angle neutron scattering diffractometer at the NIST Center for Neutron Research at the National Institute of Standards and Technology in Gaithersburg, MD.[26] The entire Q-range was acquired by collecting SANS profiles using four configurations, where $Q = 4\pi/\lambda{\cdot}\sin(\theta)$, λ being the wavelength used and 2θ the total scattering angle. Three configurations were taken at λ = 6 Å with $\Delta\lambda/\lambda$ = 10% covering the Q-range 3×10^{-3} Å^{-1} < Q < 0.4 Å^{-1}. The Q-range 1×10^{-3} Å^{-1} < Q < 6×10^{-3} Å^{-1} was acquired at λ = 8 Å with $\Delta\lambda/\lambda$ = 10%. Samples were loaded into 1 mm path length titanium cells with quartz windows. After accounting for transmission, the data were reduced to absolute scale using the NIST provided IGOR Pro reduction macros.[27] The fuzzy core−shell sphere SANS model used in this work was a modified version of an existing model in the NIST developed IGOR Pro analysis macros and all of the SANS data were fit using the known instrument resolution.[27] The details of the model and our modifications are provided in the Supporting Information. Thin-film conductivity measurements were made by depositing PEDOT:PSS-SiO_2 particles onto prepatterned ITO substrates (Ossila) from 10 mg/mL 50/50 w/w IPA/water solutions (product #S161). Resistance measurements were made using a two-probe Agilent 34401 multimeter and converted to conductivity from the known geometry of the electrodes. Multiple devices were fabricated and representative error bars plotted as the standard deviation derived from measurements of five devices. DC conductivity measurements were made using a 25-mm-diameter parallel plate stainless steel electrodes with a gap spacing of 0.4 mm. The volume fraction of the particles was systematically varied and the conductivity measurements made across the gap using Agilent 34401 multimeter set. Data were recorded for 10 min and the resistances were calculated by averaging at steady state. Steady-state flow curves were performed for these suspensions using a TA ARES G2 rheometer. The geometry used for this investigation was a 25 mm parallel plate geometry with a gap spacing of 0.4 mm. Simultaneous dielectric spectroscopy measurements were made under steady shear using a custom Labview interface controlling an Agilent E4980 LCR meter with the electrodes connected to the rotating element using a TA Instruments Dielectric Accessory modified with an electrical slip-ring (Fabricast).

ASSOCIATED CONTENT

Supporting Information

The Supporting Information is available free of charge on the ACS Publications website at DOI: 10.1021/acsami.6b07372.

Analysis of the PSS properties, adsorption of the PSS to cationic silica, and synthesis of the conductive particles over a range of process parameters along with a description of the scattering model used (PDF)

DOI: 10.1021/acsami.6b07372
ACS Appl. Mater. Interfaces 2016, 8, 24089−24096

AUTHOR INFORMATION

Corresponding Author

*E-mail: Paul.Butler@nist.gov. Phone: 301-975-2028.

Author Contributions

The manuscript was written through contributions of all authors. All authors have given approval to the final version of the manuscript.

Notes

The authors declare no competing financial interest.

ACKNOWLEDGMENTS

The authors would like to acknowledge the NIST Center for Neutron Research CNS cooperative agreement number #70NANB12H239 grant for partial funding during this time period as well as the National Research Council for support. A.S. acknowledges partial funding support from the National Science Foundation under Agreement No. DMR-1508249. The authors would also like to acknowledge the contributions of Cedric Gagnon for assistance in modification of the ARES G2 rheometer for steady-shear electrical measurements. Certain commercial equipment, instruments, or materials are identified in this paper in order to specify the experimental procedure adequately. Such identification is not intended to imply recommendation or endorsement by the National Institute of Standards and Technology, nor is it intended to imply that the materials or equipment identified are necessarily the best available for the purpose.

REFERENCES

(1) Yang, Z.; Zhang, J.; Kintner-Meyer, M. C. W.; Lu, X.; Choi, D.; Lemmon, J. P.; Liu, J. Electrochemical Energy Storage for Green Grid. *Chem. Rev.* **2011**, *111*, 3577−3613.

(2) Duduta, M.; Ho, B.; Wood, V. C.; Limthongkul, P.; Brunini, V. E.; Carter, W. C.; Chiang, Y.-M. Semi-Solid Lithium Rechargeable Flow Battery. *Adv. Energy Mater.* **2011**, *1*, 511−516.

(3) Chiang, Y.-M. Materials Science. Building a Better Battery. *Science* **2010**, *330*, 1485−1486.

(4) Campos, J. W.; Beidaghi, M.; Hatzell, K. B.; Dennison, C. R.; Musci, B.; Presser, V.; Kumbur, E. C.; Gogotsi, Y. Investigation of Carbon Materials for Use as a Flowable Electrode in Electrochemical Flow Capacitors. *Electrochim. Acta* **2013**, *98*, 123−130.

(5) Presser, V.; Dennison, C. R.; Campos, J.; Knehr, K. W.; Kumbur, E. C.; Gogotsi, Y. The Electrochemical Flow Capacitor: A New Concept for Rapid Energy Storage and Recovery. *Adv. Energy. Mater.* **2012**, *2*, 895−902.

(6) Petek, T. J.; Hoyt, N. C.; Savinell, R. F.; Wainright, J. S. Characterizing Slurry Electrodes Using Electrochemical Impedance Spectroscopy. *J. Electrochem. Soc.* **2016**, *163*, A5001−A5009.

(7) Reyes-Reyes, M.; Cruz-Cruz, I.; López-Sandoval, R. Enhancement of the Electrical Conductivity in PEDOT: PSS Films by the Addition of Dimethyl Sulfate. *J. Phys. Chem. C* **2010**, *114*, 20220−20224.

(8) Vaynberg, K. A.; Wagner, N. J.; Sharma, R. Polyampholyte Gelatin Adsorption to Colloidal Latex: pH and Electrolyte Effects on Acrylic and Polystyrene Latices. *Biomacromolecules* **2000**, *1*, 466−472.

(9) Krishnamurthy, L.; Weigert, E. C.; Wagner, N. J.; Boris, D. C. The Shear Viscosity of Polyampholyte (Gelatin) Stabilized Colloidal Dispersions. *J. Colloid Interface Sci.* **2004**, *280*, 264−275.

(10) Xie, F.; Nylander, T.; Piculell, L.; Utsel, S.; Wågberg, L.; Åkesson, T.; Forsman, J. Polyelectrolyte Adsorption on Solid Surfaces: Theoretical Predictions and Experimental Measurements. *Langmuir* **2013**, *29*, 12421−12431.

(11) Chodanowski, P.; Stoll, S. Polyelectrolyte Adsorption on Charged Particles: Ionic Concentration and Particle Size Effects - a Monte Carlo Approach. *J. Chem. Phys.* **2001**, *115*, 4951−4960.

(12) McFarlane, N. L.; Wagner, N. J.; Kaler, E. W.; Lynch, M. L. Poly(ethylene Oxide) (PEO) and Poly(vinyl Pyrolidone) (PVP) Induce Different Changes in the Colloid Stability of Nanoparticles. *Langmuir* **2010**, *26*, 13823−13830.

(13) Baier, M. C.; Huber, J.; Mecking, S. Fluorescent Conjugated Polymer Nanoparticles by Polymerization in Miniemulsion. *J. Am. Chem. Soc.* **2009**, *131*, 14267−14273.

(14) Manning, G. S. Limlting Laws and Counterion Condensation in Polyelectrolyte Solutions, 7. Electrophoretic Mobility and Conductance '. *J. Phys. Chem.* **1981**, *85*, 1506−1515.

(15) Stieger, M.; Richtering, W.; Pedersen, J. S.; Lindner, P. Small-Angle Neutron Scattering Study of Structural Changes in Temperature Sensitive Microgel Colloids. *J. Chem. Phys.* **2004**, *120*, 6197−6206.

(16) Pedersen, J. S. Analysis of Small-Angle Scattering Data from Colloids and Polymer Solutions: Modeling and Least-Squares Fitting. *Adv. Colloid Interface Sci.* **1997**, *70*, 171−210.

(17) Feigin, L. A.; Svergun, D. I. Structure Analysis by Small-Angle X-Ray and Neutron Scattering. *Acta Polym.* **1989**, *40*, 224.

(18) Lindner, P., Zemb, T. *Neutrons, X-Rays and Light: Scattering Methods Applied to Soft Condensed Matter*; North-Holland, 2002.

(19) Yi, J. Y.; Choi, G. M. Percolation Behavior of Conductor-Insulator Composites with Varying Aspect Ratio of Conductive Fiber. *J. Electroceram.* **1999**, *3*, 361−369.

(20) Takeda, Y.; Katsuta, K.; Inoue, Y.; Hakushi, T. A Conductance Study of 1:1 Complexes of 15-Crown-5, 16-Crown-5, and Benzo-15-Crown-5 with Alkali Metal Ions in Nonaqueous Solvents. *Bull. Chem. Soc. Jpn.* **1988**, *61*, 627−632.

(21) Bordi, F.; Colby, R. H.; Cametti, C.; De Lorenzo, L.; Gili, T. Electrical Conductivity of Polyelectrolyte Solutions in the Semidilute and Concentrated Regime: The Role of Counterion Condensation. *J. Phys. Chem. B* **2002**, *106*, 6887−6893.

(22) Kirkpatrick, S. Percolation Ancl Conduction. *Rev. Mod. Phys.* **1973**, *45*, 574−588.

(23) Pelster, R.; Simon, U. Nanodispersions of Conducting Particles: Preparation, Microstructure and Dielectric Properties. *Colloid Polym. Sci.* **1999**, *277*, 2−14.

(24) Niu, R.; Gong, J.; Xu, D.; Tang, T.; Sun, Z. Colloids and Surfaces A: Physicochemical and Engineering Aspects Rheological Properties of Ginger-like Amorphous Carbon Filled Silicon Oil Suspensions. *Colloids Surf., A* **2014**, *444*, 120−128.

(25) Makino, K.; Ohshima, H. Electrophoretic Mobility of a Colloidal Particle with Constant Surface Charge Density. *Langmuir* **2010**, *26*, 18016−18019.

(26) Glinka, C. J.; Barker, J. G.; Hammouda, B.; Krueger, S.; Moyer, J. J.; Orts, W. J. The 30 M Small-Angle Neutron Scattering Instruments at the National Institute of Standards and Technology. *J. Appl. Crystallogr.* **1998**, *31*, 430−445.

(27) Kline, S. R. Reduction and Analysis of SANS and USANS Data Using IGOR Pro. *J. Appl. Crystallogr.* **2006**, *39*, 895−900.

DOI: 10.1021/acsami.6b07372
ACS Appl. Mater. Interfaces 2016, 8, 24089−24096